Published by :
https://www.ijert.org/
An International Peer-Reviewed Journal

International Journal of Engineering Research & Technology (IJERT)
ISSN: 2278-0181
Vol. 15 Issue 01 , January - 2026

Bandgap Engineering of GaAs, InAs, and InSb Quantum Dots for Narrow-Bandgap Devices

G. C. Ogbu[1], O. K. Asielue [2], N.N. Tasie[3], C.I. Elekalachi[4], S. C. Igbokwe[5], E. I. Achuka[6]

[1]*Department of Industrial Physics, Enugu State University of Science and Technology.*
[2]*Department of Science Laboratory Technology Delta State Polytechnic Ogwashi.*
[3]*Department of Physics, Rivers State University*
[4]*Department of Industrial Physics, Chukwuemeka Odimegwu Ojuchukwu University.*
[5]*Department of Physics, Kingsley Ozumba Mbadiwe University, Ogboko Ideato, Imo State*
[6]*Department of Physics, Kingsley Ozumba Mbadiwe University, Ogboko Ideato, Imo State*

Abstract – *This study investigates the bandgap engineering of GaAs, InAs, and InSb quantum dots (QDs) for narrow-bandgap device applications using the Effective Mass Approximation (EMA) model. It analyzes how quantum confinement modifies the bandgap as the QD radius varies from the strong confinement regime (1–2 nm) to the weak confinement regime (6–8 nm). The results show a pronounced increase in bandgap energy with decreasing radius, driven by enhanced carrier confinement and stronger electron–hole localization at the nanoscale. Among the three materials, InSb QDs exhibit the smallest bandgaps, highlighting their potential for infrared photodetectors and long-wavelength optoelectronic systems. InAs QDs display intermediate bandgap values, making them suitable for near-infrared detection and high-efficiency photovoltaic devices. GaAs QDs maintain the largest bandgaps over the same size range, supporting applications in visible to near-infrared emitters and sensors. Overall, the findings demonstrate that precise size control enables effective bandgap tuning in III–V semiconductor QDs and confirm that the EMA model provides a reliable framework for predicting their size-dependent electronic properties.*

Keywords - Quantum dot, exciton Bohr radius, semiconductor nanostructures, confinement

1. Introduction

Quantum dots (QDs) are semiconductor nanocrystals whose electronic and optical properties can be precisely tuned through controlled variation of their size, shape, and composition. Owing to their three-dimensional quantum confinement, QDs exhibit discrete energy levels and size-dependent bandgaps, enabling their integration into a wide range of optoelectronic and photonic devices (Alivisatos, 1996; Bimberg et al., 1999). Among the materials used for QD fabrication, III–V semiconductors such as gallium arsenide (GaAs), indium arsenide (InAs), and indium antimonide (InSb) are especially attractive due to their high carrier mobilities, direct bandgaps, and strong suitability for infrared and near-infrared applications (Vurgaftman et al., 2001; Singh, 2010).

Engineering the bandgap of these materials through controlled adjustment of the QD radius is essential for developing high-performance narrow-bandgap devices, including infrared photodetectors, low-threshold lasers, and high-efficiency multi-junction solar cells (Nozik, 2002; Sargent, 2005). Narrow-bandgap semiconductors are capable of absorbing long-wavelength photons, thereby enhancing infrared sensitivity and improving utilization of the solar spectrum (Green et al., 2014). As QD size decreases, however, quantum confinement becomes increasingly dominant, producing a blue-shift (increase) in the bandgap energy. Accurate modeling of this effect is critical for achieving tailored device characteristics (Efros & Rosen, 2000; Klimov, 2007).

At room temperature, GaAs, InAs, and InSb possess bulk bandgaps of 1.42 eV, 0.36 eV, and 0.17 eV, respectively (Vurgaftman et al., 2001). Their intrinsically low bandgaps make them prime candidates for infrared and near-infrared technologies. InSb, in particular, combines an extremely narrow bandgap with a very low electron effective mass, resulting in pronounced quantum confinement effects even at relatively large radii. Consequently, small variations in size can produce substantial bandgap modulation (Sablon et al., 2011; Wang et al., 2015).

To analyze size-dependent bandgap behavior, several theoretical models have been developed. Among these, the Effective Mass Approximation (EMA), first formalized by Brus (1984), remains widely used due to its analytical simplicity and its ability to capture dominant confinement trends. EMA models the electron and hole as quasi-free particles with material-specific effective masses, confined within a spherical potential well of radius R. This approach incorporates key parameters such as effective masses and dielectric constants to estimate quantized energy levels (Harrison, 2005; Singh, 2010). Although simplified, EMA has demonstrated strong agreement with experimental data for

International Journal of Engineering Research & Technology (IJERT)
ISSN: 2278-0181
Vol. 15 Issue 01 , January - 2026

many semiconductor nanocrystals, particularly when the QD radius exceeds the exciton Bohr radius (Yu et al., 2003; Grundmann, 2010).

This study applies the EMA model to GaAs, InAs, and InSb quantum dots to theoretically evaluate the variation of their bandgap energy as a function of radius. The aim is to provide fundamental insights into how quantum confinement governs the electronic structure of III–V QDs, thereby supporting the rational design of narrow-bandgap optoelectronic materials.

2. Effective Mass Approximation (EMA) Model

The Effective Mass Approximation (EMA) is a widely used theoretical framework for modeling the size-dependent electronic properties of semiconductor nanostructures (Brus, 1984; Harrison, 2005). In this approach, the electron and hole are approximated as quasi-free particles with material-specific effective masses, confined within a spherical potential well of radius R. Within the EMA framework, the dependence of the quantum dot bandgap on size can be quantitatively described by the Brus equation:

$$E_g(R) = E_{bulk} + \frac{\hbar^2\pi^2}{2R^2}\left(\frac{1}{m_e^*} + \frac{1}{m_h^*}\right) - \frac{1.8e^2}{4\pi\varepsilon_o\varepsilon_r R} \quad (1)$$

where:

$E_{g,bulk}$ is the bulk bandgap, R is the radius of the quantum dot, h is Planck's constant, me∗ and mh∗ are the electron and hole effective masses, εr is the material's relative permittivity, and the last term represents the electron–hole Coulomb interaction energy.

The first term is the intrinsic bulk bandgap, the second term is the quantum confinement (kinetic) energy, and the third is the Coulombic correction (which reduces the bandgap).

3. Materials and Methods

Material-specific parameters including bandgap energy, effective masses, and dielectric constant were incorporated into MATLAB for the simulations. The quantum dot radius (R) was varied from 1 nm to 10 nm in increments of 0.5 nm to capture the transition from the strong to weak confinement regimes. For each radius, the size-dependent bandgap Eg(R) was computed using the Brus equation, and the resulting values were plotted against radius to illustrate bandgap tuning for each material. All input parameters were obtained from empirical data reported in the scientific literature, as summarized in Table 1.

Table 1: The Group III-V QDs experimental parameters used for the study

Quantum dots	M_e^x	M_h^x	$E_{g(bulk)}$ at 300k
InAs	$0.02m_o$	$0.40m_o$	0.36eV
InSb	$0.02m_o$	$0.40m_o$	0.17eV
GaAs	$0.06m_o$	$0.51m_o$	1.42eV

4. Results and Discussion

Using the Brus equation within the Effective Mass Approximation (EMA) framework, the bandgap energies of GaAs, InAs, and InSb quantum dots (QDs) were calculated as a function of radius (R) from 1–10 nm, as shown in Figure 1. The results exhibit a strong inverse relationship between bandgap energy and QD radius for all three materials, consistent with EMA predictions. As the radius decreases, charge carriers experience enhanced spatial confinement, leading to an increase in their kinetic energy and a corresponding widening of the bandgap relative to the bulk values. This quantum confinement effect is most pronounced at radii below the exciton Bohr radius of each material

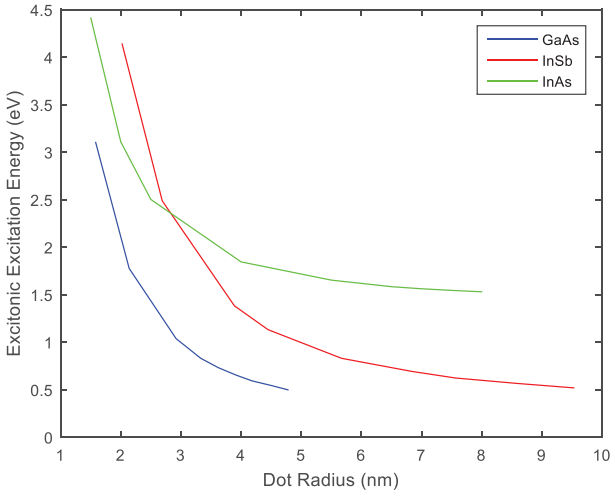

Fig. 1 Size-Dependent Bandgap of CdSe, CdS and ZnS Quantum Dots (EMA Model)

International Journal of Engineering Research & Technology (IJERT)
ISSN: 2278-0181
Vol. 15 Issue 01 , January - 2026

For GaAs quantum dots, the bandgap increases sharply from the bulk value of 1.42 eV to approximately 3.5 eV as the radius decreases to around 1 nm, shifting their optical response from the near-infrared into the ultraviolet region. As the radius increases to about 3–5 nm, the bandgap gradually decreases to roughly 2.0 eV, bringing their absorption and emission into the visible spectrum. At radii above 8–10 nm, the bandgap approaches the bulk value, indicating the onset of the weak confinement regime. These trends demonstrate that GaAs QDs are highly tunable across a wide energy range and are therefore more suitable for visible or ultraviolet optoelectronic applications such as quantum dot lasers and LEDs rather than for narrow-bandgap infrared devices.

For InAs quantum dots, the bandgap rises from the bulk value of 0.36 eV to roughly 1.6 eV at a radius of 1 nm, shifting their response from the mid-infrared to the visible region. In the 3–5 nm range, the bandgap decreases to approximately 0.5–0.6 eV, entering the near-infrared regime, and eventually converges toward the bulk value beyond 8–10 nm. This strong size-dependent tunability within the infrared region makes InAs QDs highly suitable for narrow-bandgap technologies such as infrared photodetectors, quantum dot solar cells, and low-bandgap laser devices.

For InSb quantum dots with an extremely low bulk bandgap of 0.17 eV, the relative confinement-induced shift is particularly large. At a radius of 1 nm, the bandgap increases to about 1.2 eV, placing their response in the near-infrared. As the radius increases to 3–5 nm, the bandgap decreases to around 0.4–0.6 eV, and approaches the bulk value beyond approximately 8 nm. Owing to both their naturally low bulk bandgap and the significant tunability introduced by quantum confinement, InSb QDs are especially well-suited for long-wavelength infrared applications such as thermal imaging sensors, infrared detectors, and thermophotovoltaic devices.

Overall, the results show that although all three materials follow the expected 1/R2 dependence at small radii, GaAs QDs are more appropriate for high-energy visible and ultraviolet applications, whereas InAs and InSb QDs are better aligned with narrow-bandgap infrared technologies. Their strong size-dependent tunability allows InAs and InSb QDs to achieve bandgaps across the 0.2–1.2 eV range, which is particularly advantageous for infrared optoelectronics.

5. Conclusion

This study demonstrates the feasibility of bandgap engineering in GaAs, InAs, and InSb quantum dots using the Effective Mass Approximation (EMA) to describe the relationship between particle radius and bandgap energy. The results confirm that decreasing the QD radius intensifies quantum confinement, leading to a substantial increase in bandgap energy, while increasing the radius reduces the confinement effect and causes the bandgap to approach the bulk value.

Among the materials studied:

- **InSb QDs** exhibit the lowest bandgaps, making them ideal for long-wavelength and infrared applications where minimal bandgap is advantageous.
- **InAs QDs** display intermediate bandgap values, offering a balance between tunability and infrared sensitivity, well suited for near-infrared photodetectors and photovoltaic devices.
- **GaAs QDs** maintain the highest bandgap values across the same size range, aligning them with visible to near-infrared applications that require higher-energy transitions.

Overall, the findings confirm that the bandgap tunability of III–V semiconductor quantum dots can be precisely controlled through nanoscale size engineering. The EMA framework provides a robust theoretical basis for predicting and tailoring QD electronic properties, supporting the design of next-generation optoelectronic and photonic devices.

References

[1] Alivisatos, A. P. (1996). Semiconductor clusters, nanocrystals, and quantum dots. *Science, 271*(5251), 933–937.

[2] Bimberg, D., Grundmann, M., & Ledentsov, N. N. (1999). *Quantum Dot Heterostructures*. John Wiley & Sons.

[3] Vurgaftman, I., Meyer, J. R., & Ram-Mohan, L. R. (2001). Band parameters for III–V compound semiconductors. *Journal of Applied Physics, 89*(11), 5815–5875.

[4] Singh, J. (2010). *Semiconductor Optoelectronics: Physics and Technology*. McGraw-Hill.

[5] Nozik, A. J. (2002). Quantum dot solar cells. *Physica E: Low-dimensional Systems and Nanostructures, 14*(1–2), 115–120.

[6] Sargent, E. H. (2005). Infrared photovoltaics made by solution processing. *Nature Photonics, 1*(1), 1–2.

[7] Green, M. A., Emery, K., Hishikawa, Y., Warta, W., & Dunlop, E. D. (2014). Solar cell efficiency tables (version 43). *Progress in Photovoltaics, 22*(1), 1–9.

[8] Efros, A. L., & Rosen, M. (2000). The electronic structure of semiconductor nanocrystals. *Annual Review of Materials Science, 30*(1),

International Journal of Engineering Research & Technology (IJERT)
ISSN: 2278-0181
Vol. 15 Issue 01 , January - 2026

475–521.

[9] Klimov, V. I. (2007). *Nanocrystal Quantum Dots*. CRC Press.

[10] Sablon, K. A., Little, J. W., Sergeev, A., Mitin, V., Vagidov, N., & Stroscio, M. A. (2011). Strong enhancement of solar cell efficiency due to quantum dots with built-in charge. *Nano Letters, 11*(6), 2311–2317.

[11] Wang, X., Ren, X., Kahen, K., Hahn, M. A., Rajeswaran, M., Maccagnano-Zacher, S., ... & Peng, X. (2015). Non-blinking semiconductor nanocrystals. *Nature, 459*(7247), 686–689.

[12] Yu, P. Y., & Cardona, M. (2003). *Fundamentals of Semiconductors: Physics and Materials Properties* (3rd ed.). Springer.